COMOTI
ROMANIAN RESEARCH & DEVELOPMENT INSTITUTE FOR GAS TURBINES

TURBO

Scientific Journal

vol. VI (2019), no. 1

The international Air Show in Paris was organized by SIAE, a subsidiary of GIFAS, the French Aerospace Industry Association.

The 53rd edition took place at the Le Bourget Exhibition Park on 17-23 June 2019 and again brought together all the players in this global industry around the latest technological innovations.

The International Paris Air Show was a special time for every business, an opportunity in the space of one week to meet all the main industry players, seize new business opportunities, present expertise and innovations to the world and forge technology partnerships.

EDITORIAL

Fundamentele creativității inventive (1)

Legătura de rudenie dintre artă și știință o onorează și pe una și pe cealaltă: e un titlu de glorie pentru știință de a putea oferi frumuseții principalele sale puncte de sprijin, e un titlu de glorie pentru artă de a-și baza cele mai măreațe opere de artă pe adevărul științei.

Hippolyte Taine

Cunoașterea este parcursul gândirii umane de la ignoranță la adevăr iar baza cunoașterii este reflectarea realității obiective în mintea omului, prin prisma activităților practice. Astfel activitatea cognitivă umană este condiționată de practică și este dominată de stăpânirea practică a realității. Procesul acesta este perpetuu, dialectica cunoașterii fiind exprimată în contradicția dintre complexitatea nelimitată a realității obiective și limitarea cunoștințelor noastre. Calea cunoașterii este calea de la contemplație la gândirea abstractă, iar procesul cunoașterii este unul viu, dezvoltarea științei începând prin colectarea faptelor, ce pot fi sistematizate pe baza conceptelor ca elemente structurale având drept axe principiile, postulatele/axiomele. Prin principiu se înțelege poziția inițială a oricărei ramuri a științei, cum sunt axiomele geometriei euclidiene ori postulatul lui Niels Bohr în mecanica cuantică.

Știința este principala formă a cunoașterii umane iar impactul său asupra condițiilor reale ale vieții cotidiene este semnificativ. Sub acest impact trebuie să navigăm și să acționăm, spre cele mai semnificative, durabile, repetitive și obiective conexiuni interne în natură, societate și gândire, care apar sub forma unui raport între concepte ori categorii.

Dezvoltarea de noi cunoștințe se realizează prin utilizarea pe scară largă a metodelor științifice generale în cercetarea teoretică și experimentală. Metoda este și un instrument pentru rezolvarea principalei sarcini a științei: descoperirea unor legi obiective ale realității și totodată determină necesitatea și locul aplicării analizei și sintezei, inducției și deducerii, comparării studiilor teoretice și experimentale. Acesta este un instrument de gândire al cercetătorului pentru a rezolva o problemă și pentru a formula o idee în procesul de rezolvare a problemei.

Viziunea filozofică a lumii implică o serie de idei despre ce este știința, cum funcționează și cum se dezvoltă, ce poate și ce nu poate fi disponibil pentru cercetare. Filozofii din trecut au făcut multe predicții despre importanța crescândă a științei, însă nu și-au putut imagina impactul masiv, neașteptat și chiar dramatic al realizărilor științifice și tehnice asupra vieții. A existat o luptă asiduuă între teologie și știință.

EDITORIAL

Fundamentele creativității inventive (2)

În Evul Mediu, teologia a câștigat treptat o poziție dominantă ce-i dădea dreptul de a discuta și de a rezolva problema indigenilor lumii, problema structurii universului și locul omului în univers, semnificația și valorile superioare ale vieții.

A trebuit să treacă mult timp, să se succeadă episoade dramatice precum arderea pe rug a lui Giordano Bruno ori retractarea teoriei heliocentrismului și arestul la domiciliu al lui Galileo Galilei, despre care Stephen Hawking spunea că, poate mai mult decât orice altă persoană, a fost responsabil pentru nașterea științei moderne, înainte ca rolul științei să devină decisiv în ideologia esențială și a fost necesar un timp îndelungat pentru ca răspunsurilor științifice la întrebări să devină elemente ale educației generale.

Secolul XX a fost secolul victoriei revoluției științifice. Spre sfârșitul său și până astăzi tranziția continuă spre economia informației, bazată pe toate schimbările datorate științei și tehnologiei căci omenirea nu doar crede ci își pune speranțe în capacitatea științei de a rezolva problemele globale și, în consecință, de a îmbunătăți calitatea vieții. Această încredere se reflectă în domeniile culturii și gândirii sociale, precum explorarea spațiului, creația, energia nucleară. Credința în inevitabilitatea progresului științific, tehnic și social, a determinat soluții pentru probleme precum cele de mediu, dezastre, foamete, boli etc.

În timp s-au clarificat două abordări principale ale cercetării științifice. Primul tip de abordare îi aparține chiar lui Galileo, anume că scopul științei este de a stabili ordinea care stă la baza fenomenelor prin care trebuie reprezentate posibilitățile obiectelor și descoperirea unor noi fenomene. Aceasta se numește cunoaștere teoretică sau "știință pură".

A doua abordare îi aparține filozofului elisabetan Francis Bacon, în epoca nașterii științei moderne, contestatar al scolasticii sterile: *Lucrez pentru a pune bazele viitoarei prosperități și puteri ale umanității. Pentru a atinge acest scop, propun o știință abilă nu în disputele școlare, ci în inventarea noilor meșteșuguri.*

Știința astăzi se află pe acestă cale, cea a îmbunătățirii tehnologice a practicii, căci inovația în practică a devenit un atribut al timpului.

Autor: Elena Banea

Iulie 2019

EDITORIAL

Fundamentals of Inventive Creativity (1)

The kinship between art and science honours them both: there is a title of glory for science to be able to provide its main counterforts to beauty, as well as there is a title of glory for art to rely on science as regards its most valuable masterpieces.

Hippolyte Taine

Knowledge represents the process of human thinking from ignorance to truth, while the basis of knowledge is the reflection of objective reality into human mind through practical activities. Thus, human cognitive activity is conditioned by practice and prioritized by practical ruling of reality. This is a continuous process, knowledge dialectics expressing itself out of a contradiction between the major complexity of objective reality and our limited knowledge. The knowledge path is the way from contemplation to abstract thinking and the knowledge process is in continuous evolution, as science development starts from data collection that can be systematized on the basis of concepts perceived as structural elements that rely on principles, postulates/axioms. A principle represents the initial stage of any branch of knowledge, such as Euclid's geometry axioms or Niels Bohr's postulate in quantic mechanics.

Science is the main form of human knowledge and its impact on the real conditions of everyday life is quite significant. That is to say that one has to guide his/her path and actions according to this impact towards the most significant, lasting, repetitive and objective internal connections within nature, society and thinking, which are represented by relationships between concepts and categories.

Development of new knowledge is achieved through the use of general scientific methods on a large scale, both in theoretical and applied research. The method is also a tool for accomplishing the main target of science: the search of objective rules of reality and the identification of the need and place of the application of analysis and synthesis, induction and deduction, of comparison between theoretical and applied studies. This is a researcher's reasoning tool that helps him/her solve a problem and postulate a principle during the problem-solving process.

A philosophical vision of the world involves a series of ideas concerning the nature of science, the way it works and develops, and also what can or cannot be available to research. The philosophers of the past made many predictions about the increasing importance of science, and yet they were not able to predict the major, unexpected and even dramatic impact of the scientific and technical achievements over everyday life. There used to be a strong conflict between theology and science.

EDITORIAL

Fundamentals of Inventive Creativity (2)

During the Middle Ages, theology gradually achieved a dominant position that allowed it to discuss and resolve the issue of the indigene populations worldwide and of various other aspects, such as the structure of the universe and man's place in the universe or the significance and major values in life.

A long time had to pass, dramatic episodes to succeed, such as Giordano Bruno's public execution or Galileo Galilei's retraction of his heliocentric theory and his domestic arrest, a personality about whom Stephen Hawking said that "he was responsible, more than any other person, with the birth of modern science", before the role of science to become decisive for essential ideology and long before the answers to scientific questions to become part of the general education.

The XXth century represented a century of triumph of scientific revolution. Towards its end and up to these days a continuous transition took place towards an information economy, which is based on all the changes owed to science and technology, as humankind not only believes, but also relies on the science capacity to solve global issues and, therefore, to improve the quality of life. This reliance is reflected in the fields of culture and social reasoning, such as space exploration, creation or nuclear power. Belief in the inevitability of scientific, technical and social progress triggered solutions to such issues as environment, disasters, famine, diseases, etc.

Two main approaches of scientific research have outlined in time. The first one belongs to Galileo himself, and it refers to the fact that the aim of science is that of establishing the order that fundaments the phenomena by means of which the potential of objects must be represented and also the discovery of new phenomena. This is to be called theoretical research or "sheer science".

The second approach belongs to the Elizabethan philosopher Francis Bacon, during the epoch of modern science birth, an opponent of sterile scholastics: *"I strive towards laying the foundations of future prosperity and power of mankind. In order to achieve this, I suggest a certain kind of science keen not in scholar disputes, but in contriving of new crafts."*

Today's science is following that very path, that of technological improvement in experimentation, since experimental innovation has become a current characteristic of the day.

Author: Elena Banea

July 2019

More information regarding the scientific journal can be found at:
http://www.comoti.ro/ro/jurnalul_stiintific_turbo.html
turbojournal@comoti.ro
jeni.popescu@comoti.ro

ISSN: 2559-608X
ISSN-L: 1454-2897
Scientific Journal TURBO is included in ICI World of Journals:
https://journals.indexcopernicus.com/search/details?id=48512
ICV 2017: 41.25

TABLE CONTENT

PRELIMINARY COMBUSTION TESTS OF A NEW COMBUSTOR SECTOR CONCEPT

Andreea MANGRA[1], Florin FLOREAN[1], Cornel SANDU[1], Marius ENACHE[1], Razvan CÂRLĂNESCU[1], Radu KUNCSER[1]

ABSTRACT: Efficient combustion is the key integral part in power generation related sectors like gas turbine, aircraft engines and industrial burners wherein diffusion flame has long been in use. The paper presents the experimental program, data acquisition and analyses of a new RQL combustor sector concept geometry. Combustor parameters have been monitored and recorded. Optimal flame stabilization, combustion, cooling air distribution and fuel atomization improve combustion efficiency.

KEYWORDS: RQL Combustor, Combustor Testing, testing rig, flame stability

1. INTRODUCTION

The Rich burn - Quick mix - Lean burn (RQL) combustor, which is the focus of the present paper, is one of the most promising NOx reduction concept studied. The RQL combustor concept was introduced in the 80s [1], and later, in the 90s, has been pursued by the National Aeronautics and Space Administration (NASA) [2] as a technology aimed to decrease the level of NOx emissions from gas turbine engines. The key factor for reducing NOx emissions is to diminish the maximum flame temperature, thus inhibiting the dissociation of the Nitrogen molecules in the air, and consequently decreasing the reaction rates for the formation of Nitrogen oxides via the thermal NOx production mechanism [3]. To this purpose, the RQL combustor creates a fuel rich mixture in the upstream region of the combustor (the Rich burn region). The excess amount of fuel absorbs part of the heat of reaction decreasing the gas temperature in the region. The reason for employing excess fuel to decrease the temperature instead of using excess air is the enhanced stability of the rich flames, reducing the likelihood of flame blow-off during operation [4]. Furthermore, the lack of Oxygen in the region further limits the NOx formation rates, the peak of NOx formation occurring on the fuel lean side of the stoichiometric mixture [5]. It was also observed that fuel rich combustion conditions tend to inhibit both the reactivity of the fuel bound Nitrogen [6] and the rate of ammonia conversion to NO_3 [4]. The effectiveness and efficiency of combustion is highly dependent on the degree of atomization and on the uniformity of its mixing in the Fuel rich zone. The air used for atomization may be brought into the Fuel rich zone after flowing over the outside of the liner wall, such that to provide cooling to the Fuel rich zone liner. This is particularly important since conventional film cooling in this region may create local near-stoichiometric mixtures that would produce high levels of NOx [5]. In order to conduct the experimental campaign an instrumentation scheme is created, to control and monitor the RQL combustor, and a starting sequence with all the parameters that are involved the process.

2. THE TESTING RIG

2.1 Control, monitor and data acquisition system

The combustor starting is carry out using the testing rig operating system, composed of a data acquisition system and a programmable controller which have been adapted for these experiments. Two parameters visualization screens have been created.

[1] National Research and Development Institute for Gas Turbines COMOTI, Bucharest, Romania

2.2 Air preheating line

In order to deliver the air at the desired temperature at the combustion chamber inlet, a pre-heater has been used (fig. 2 a)). The pipes between the pre-heater and the experimental combustion chamber assembly have been thermally insulated to minimize the heat losses. A special section has been added before the experimental combustion chamber with the purpose to stabilize and smoothen the air flow. The air temperature, pressure and mass flow rate have been monitored before combustion chamber entrance. The diagram of the air preheating line is presented in fig. 2 b).

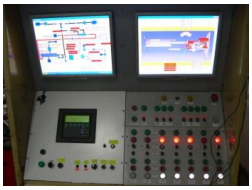

Fig. 1 Control and data acquisition system

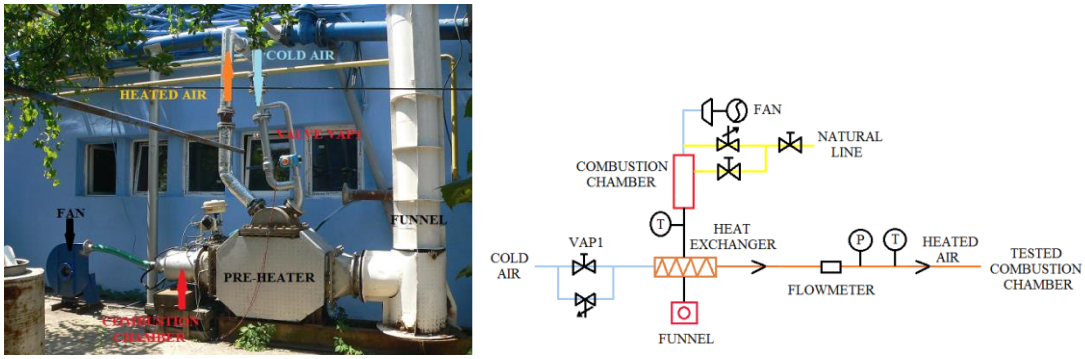

a) b)

Fig. 2 a) The air pre-heater b) air preheating line diagram

2.3 Fuel supplying line

The fuel is led from the main tank, using a pre-fed fuel pump, through a 10 μm filter. Because of the large distance from the tank to the testing rig, a second fuel pump has been installed closer to combustion chamber assembly. The fuel than enters the injectors through SV2 valve. The used injectors are spill return pressure atomizers. A part of the fuel is atomized in the combustion chamber, and another part returns in the fuel tank via SV1 valve, depending on the functioning regime. The fuel warms up in the injectors, thus in order to cool down the fuel which returns to the fuel tank via the SV1 valve a coil was used. The fuel pressure is monitored using manometers. One manometer is positioned on the direct fuel pipe, before SV2 valve. Another manometer is positioned on the return fuel pipe line, after the coil. The fuel injection pressure is controlled by varying the amount of fuel that returns to the fuel tank using a manual tap. To stop the fuel feeding, valves SV1 and SV2 are closed and the bypass valve SV3 is opened.The fuel supplying system is presented schematically in fig. 3.

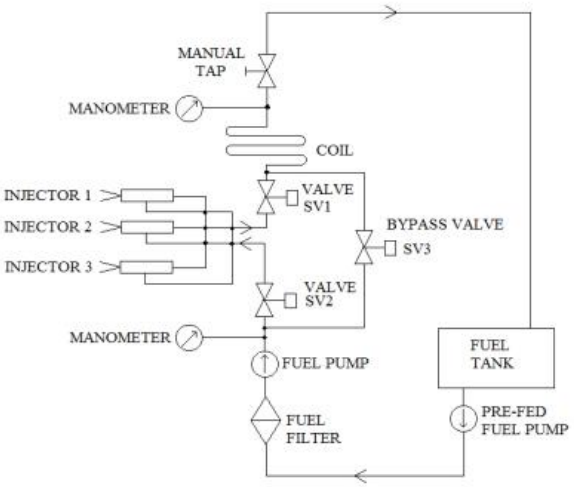

Fig. 3 Diagram of the fuel supply system

Tests to determine the fuel flow through the injectors, function on the fuel pump regime have been conducted before starting the combustion tests. The results are presented in section 3.

2.4 Combustion chamber assembly

The tested combustion chamber represents a quarter of an annular type combustion chamber. It is equipped with 3 injectors functioning on kerosene. The fire tube and fuel injectors have been delivered by our consortium partners.
In fig. 4 a) - b) the fire tube and a section through the combustion chamber CAD model is presented, to better understand the way it works. The geometrical data is copyright protected, thus more details can not be provided.

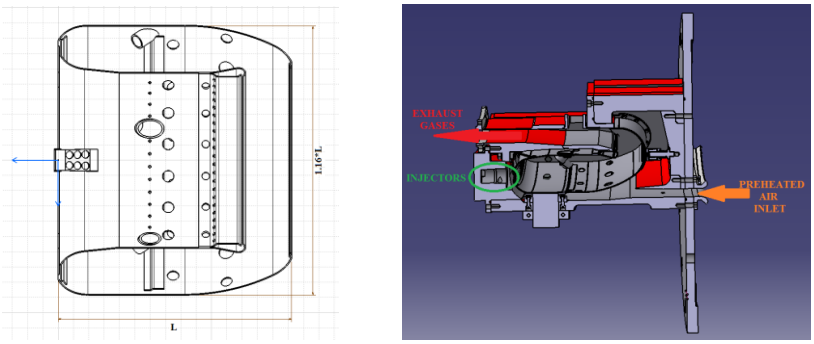

a) b)

Fig. 4: a) the fire tube; b) section through the combustion chamber CAD model

The combustion chamber is equipped with a quartz window in order to view the flame and observe if the combustion process is stable. The exhaust gases temperature has been monitored at the combustion chamber exit with the help of 3 thermocouples. In order to protect the side walls from the high temperatures obtained during combustion, they were designed with an interior channel through which cooler air is circulated. The cooling air is taken from the air pipe line through a flexible hose (fig. 5), before the flow-meter thus not influencing the air mass flow that enters the combustion chamber, and returned in the exhaust gases flow after the thermocouples that monitor the exhaust gases temperature, thus not influencing the temperature.
A counter pressure valve was placed on the outlet section to simulate the turbine stator.

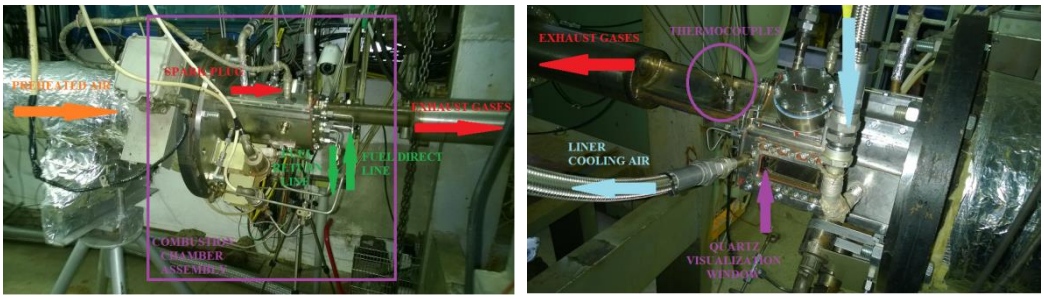

Fig. 5 Combustion chamber assembly on the testing line

The whole testing rig diagram is presented in fig. 6.

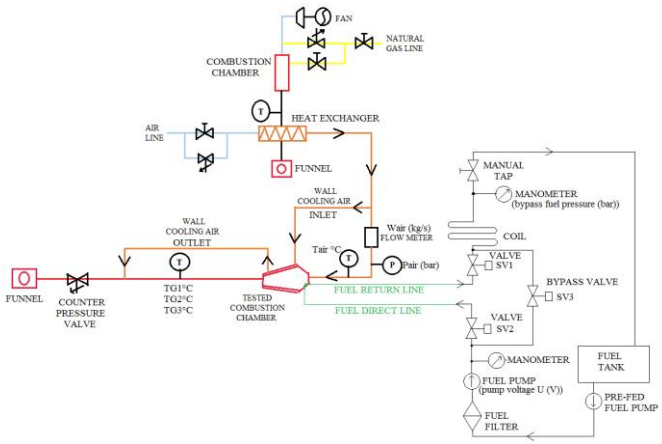

Fig. 6 Testing rig diagram

3. FUEL FLOW CHARACTERISTICS OF INJECTORS

The tested fuel injectors have been delivered by our consortium partners. Before starting the combustion tests, the fuel flow characteristics of the injectors has been determined. For this purpose, a testing rig has been built, which included a max. 12 V DC fuel pump, with variable amperage and a 10-micron filter. The fuel pressure on the injectors' bypass pipe has been monitored using a pressure gauge. Also, on the injectors' bypass pipe a valve has been positioned, which by opening or closing has been used to adjust the fuel pressure. The diagram of the testing rig is presented in fig. 7.

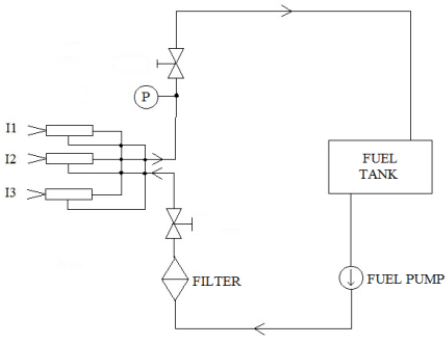

Fig. 7 Diagram of the injectors fuel flow characteristics testing rig

The volume fuel flow rates have been determined on the overall 3 injectors. Because at the time of the experiments a kerosene flow-meter was not available, the method to determine the volume flow consisted in measuring, for different fuel pump functioning regimes characterized by voltage and amperage, the fuel volume which passed through the 3 injectors in 1 minute. The measured data has been compared with the calculated fuel flow rates delivered by our consortium partners (fig. 9). The diagram in fig. 9 will help determine the fuel flow during the experiments, based on the functioning regime of the fuel pump.

Fig. 8 Fuel flow measurement

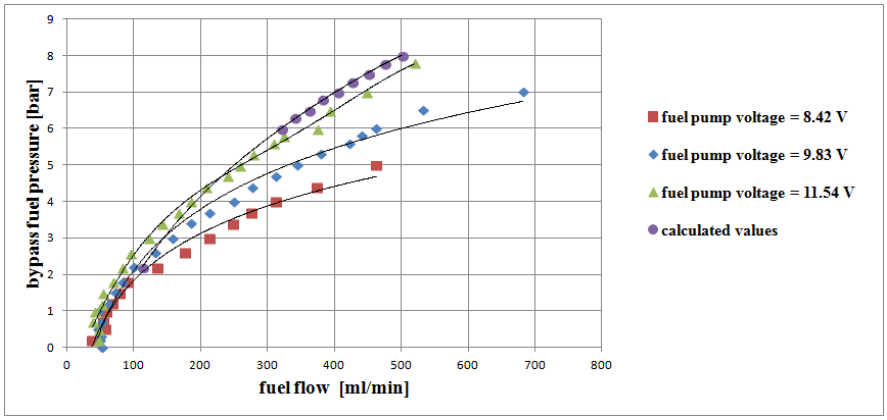

Fig. 9 Fuel flow characteristic

From fig. 9 it can be observed that by increasing the voltage of the fuel pump, thus increasing its power, the fuel flow increases, as it was expected. Also, by increasing the bypass fuel pressure a smaller quantity of fuel goes through the bypass and a larger quantity goes through the exit nozzle of the injectors, thus leading to an increase of the fuel flow that will participate in the combustion process.

4. COMBUSTION CHAMBER TESTS

A series of tests under different operating conditions, presented in Table 1, have been conducted. The objective of a measurement was to determine combustion "stable point" and the various phases of the combustion process have been identified, establishing all operational points and determining the fuel and airflow rates required to maintain combustion. This led to the completion of the experimental analysis of the new combustion chamber.

Ignition and re-ignition tests have been conducted first, as it can be seen from fig. 10. During these tests the air pressure and air mass flow rate have been varied as it can be seen from figures 11-12. From fig. 10 it can be seen that through a long period of time (2500s) the combustion chamber has been ignited and re-ignited successfully several times.

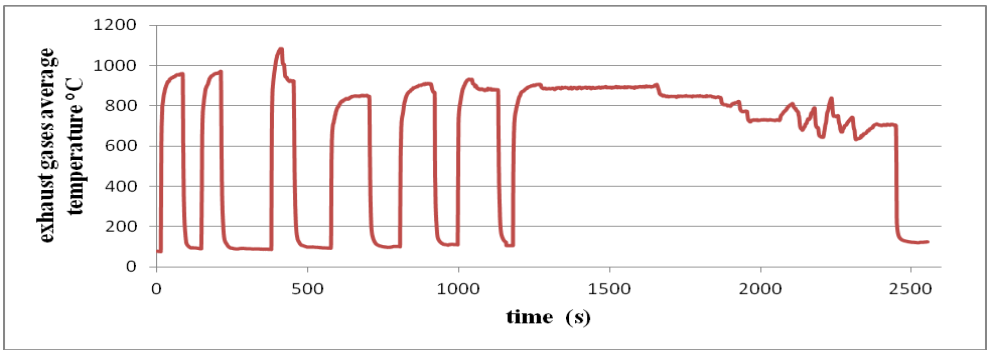

Fig. 10 Exhaust gases average temperature during ignition and re-ignition tests

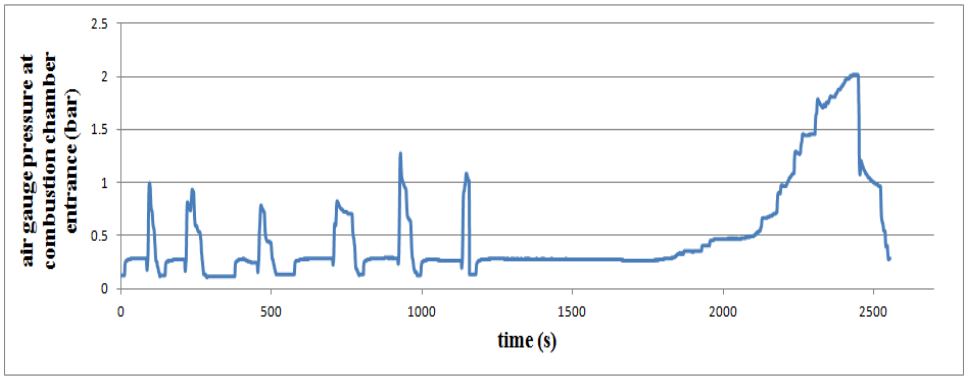

Fig. 11 Air gauge pressure during ignition and re-ignition tests

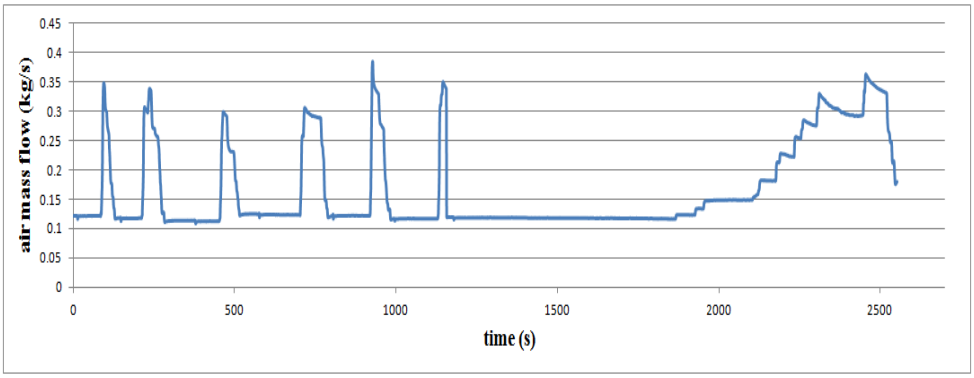

Fig. 12 Air mass flow during ignition and re-ignition tests

In the next stage of the tests, the operational regimes, presented in Table 1, have been maintained for a longer period of time. During the tests the following parameters have been monitored and registered by the data acquisition system: the air pressure, temperature and mass flow rate at the combustion chamber inlet and the exhaust gases temperature.

The total fuel volume flow rate (on all 3 injectors) has been determined using the diagram from fig. 9, having as input data the fuel pump voltage and the fuel pressure on the return line noted during the tests. The bypass fuel pressure was varied in order to obtain a fuel volume flow that in combination with the air mass flow rate led to an exhaust gases average temperature not higher than 800°C.

The values presented in Table 1 are averaged values over a period o time in which the air pressure, temperature and mass flow have been kept constant as best as possible. TG1, TG2, TG3 are the temperature values registered by the 3 thermocouples positioned at the exit of the combustion chamber assembly.

As it can be seen from fig. 8, the middle injector gives a higher fuel flow. This can explain why temperature TG2 is higher that temperatures TG1 and TG3. No component of the combustion chamber assembly has been damaged during the tests.

During the experiments at low load regimes it has been observed that visualization quartz window was partially filled with tar deposits (fig. 13). This can be explained by a poor atomization and vaporization of the fuel in these functioning regimes.

Table 1 Tested functioning regimes

Pair	Tair	Wair	U	Bypass fuel pressure	Wfuel (on 3 injectors)	TG1	TG2	TG3	TG avg.
bara	°C	kg/s	V	bar	ml/min	°C	°C	°C	°C
1.28	92	0.122	9.83	3.5	177	761	934	634	776
1.28	116	0.122	9.83	3.2	156	744	886	611	747
1.5	92	0.15	9.83	3	146	574	646	448	556
1.5	142	0.15	9.83	3	146	649	736	526	637
2.6	110	0.308	9.83	4.8	312	587	642	490	573
3.56	110	0.304	9.83	5	344	691	754	564	669
3.8	110	0.339	9.83	5.1	354	618	676	516	603
4	110	0.332	9.83	5.1	354	621	679	518	606

Fig. 13 Combustion chamber assembly during the tests

5. CONCLUSIONS

The combustor starting is carry out using the testing rig operating system, composed of a data acquisition system and a programmable controller which have been adapted for these experiments. Before starting the combustion tests, the fuel flow characteristics of the injectors has been determined. These preliminary combustion tests validated the proper functioning of the various components of the testing rig, namely: the air pre-heater, the fuel supply system, the data acquisition and monitoring system.

During the combustion tests the following parameters have been varied (air temperature, pressure and mass flow rate, the bypass fuel pressure) in order to simulate different functioning regimes. The experiments proved a good ignition and re-ignition characteristic. The functioning of the combustion chamber at low load regimes led to the formation of tar deposits. Tests at large load regimes showed a proper functioning of the combustion chamber without damage of the components.

ACKNOWLEDGEMENT

The work presented here was carried out under the European research project FP 7 Clean Sky "Efficient Systems and Propulsion for Small Aircraft" – ESPOSA, number 284859, financed by the European Commission.

REFERENCES

[1] Samuelsen, S.; 2006; The Gas Turbine Handbook, Rich burn, quick-mix, lean burn (RQL) combustor.; US Department of Energy; Office of Fossil Energy; National Energy Technology Laboratory; pp. 227-233.
[2] Rezvani, R.; 2010; A Conceptual Methodology for the Prediction of Engine Emissions; *Ph. D. Thesis*; Georgia Institute of Technology, School of Aerospace Engineering
[3] Rink, K. K., Lefebvre, A. H.; 1989; The Influence of Fuel Composition and Spray Characteristics on Nitric Oxide Formation; *Combustion, Science and Technology*,Vol. 68, pp. 1–14.
[4] Nakata, T., Sato, M., Ninomiya, T., Hasegawa, T. ; 2007; A Study of Low NOx Combustion in LBG-Fuelled 1500° C-Class Gas Turbine; Journal of Engineering for Gas Turbines and Power, vol. 118, iss. 3, pp. 534-540
[5] Martin, F.J., Dederick, P.K.J.; 1976; NOx from Fuel Nitrogen in Two-Stage Combustion, *Sixteenth Symposium (International) on Combustion*, The Combustion Institute, Pittsburgh, PA, pp. 191 - 198
[6] Snyder, T. S., Rosfjord, T. J., McVey, J. B., and Chiappetta, L. M.; 1994; Comparison of Liquid Fuel/Air Mixing and NOx Emissions for a Tangential Entry Nozzle, ASME 1994 International GAs Turbine and Aeroengine Congress and Exposition, The Hague, Netherlands

CFD ANALYSIS FOR AXIAL TURBINE PERFORMANCE MAPS ESTIMATION

NICOARĂ Răzvan[1], OLARU Daniel[1]

ABSTRACT: In this paper, the flow and performance of a small single-stage axial turbine are studied. Using the CFD numerical calculation, Computational Fluid Dynamics, the universal performance map of the tubine is determined. The map is created by succesive simulation of different cases and by using similarity parameters in order to obtain the constant mass flow curves. The results are then used to describe the performance of the turbine at different regimes. The paper will describe how the theoretical model is obtained, the numerical grid and cases, as wel as the resulted performances.

KEYWORDS: turbine, characteristics, CFD, similarity, performance

1. INTRODUCTION

The gas turbines operation is a complex process involving the simultaneous and stable deployment of compression, burning and expansion processes. The problem of operating the engine at loads other than the nominal one, the load for which it was designed, must be studied as early as the designing phase. In order to determine the behaviour of the engine at these regimes it is necessary to evaluate the performance of the component elements, this being possible by studying their performance characteristics.

The engine turbine extracts the energy from the working fluid, fluid with a high energy state. Following the combustion process, because of the heat generated, the potential energy of the fluid increases greatly while the kinetic energy remains low due to low speeds at the exist of the combustion chamber. Thus, in order to extract energy from the working fluid and to transmit that energy to a consumer, the turbine converts the potential energy into kinetic energy (in the stationary blades) and then into mechanical work (in the rotational blades).

The turbine performance map enables the estimation of performances over the entire operational range by using similarity parameters. Thus, the performances are described by three parameters: reduced speed, reduced mass flow and specific enthalpy drop.

2. THEORETICAL MODEL DESIGN

The turbine design begins by calculating the engine thermodynamic cycle to determine the input parameters, necessary power and efficiencies. Depending on these parameters and constructive aspects, the turbine type and number of stages are determined. The speed is also selected with respect to other components of the respective turbomachine, compressor, mechanical power consumers, bearings, etc. In principle, they satisfy the absolutely necessary condition of the turbine to be consistent with the other components of the turbine engine in the general architecture.

In the designing process, calculation are being conducted in order to study the flow through the stage and to determine the optimal geometry as well as resistance and vibration calculations to determine the mechanical loads and frequencies of the blades and turbine disks. Only the flow calculation will be presented in this paper.

The flow calculation is iterative, being graphically represented in Figure 1. For a single-stage turbine, it can be divided into three major steps: global calculation at mean radius, blade profiling and building the turbine performance map. For multi-stage turbines, the calculation is similar.

[1] National Research and Development Institute for Gas Turbines COMOTI, Bucharest, Romania

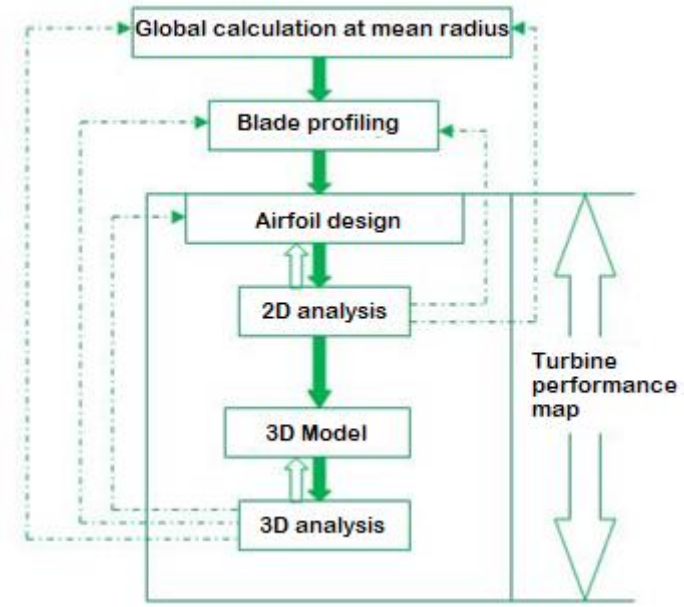

Fig. 1 The flow modeling process of the axial gas turbines [1]

The global calculation at the mean radius has the purpose of determining global geometric parameters: blade heights, angles of velocity and thermodynamic parameters corresponding to each inlet and outlet section of the stage or turbine stages. This calculation studies the flow only in the axial direction. Blade profiling adds the radial dimension, imposing a law of parameters variation, which allows the determination of flow parameters at different radius.

The turbine performance map allows the turbine to be coupled to the other elements of the turbomachinery by calculating the engine working line. It involves calculating the performance of the turbine in a wide range of operating regimes, not just the nominal one, as was done in the two previous steps. It is the most complex part of the flow modelling of a gas turbine in terms of approach possibilities.

Based on turbine geometry and the input data, a bidirectional flow analysis can be achieved using semiempirical models to determine pressure losses in the turbine stage [2]. As a result of this analysis, the performance map of the turbine can be built. Another approach involves stacking the profiles and obtaining the three-dimensional model. Further, this model is used in a CFD (Computational Fluid Dynamics) environment for a three-dimensional flow analysis. Another method of obtaining the maps for an axial gas turbine is to build the prototype and to compute it as a result of experimental measurements made at the test bench. The three methods can be used separately or combined to validate the results.

The geometry of the turbine has been designed to achieve the desired performance but also to easily fabricate the components. Thus, the velocity triangles were solved at the mean radius and profiles were defined. For constructional simplicity and due to the low height of the turbine channel, the same profile was used throughout the blade's height. Figure 2 shows the geometry of the stationary blades and the geometry of the rotational blades.

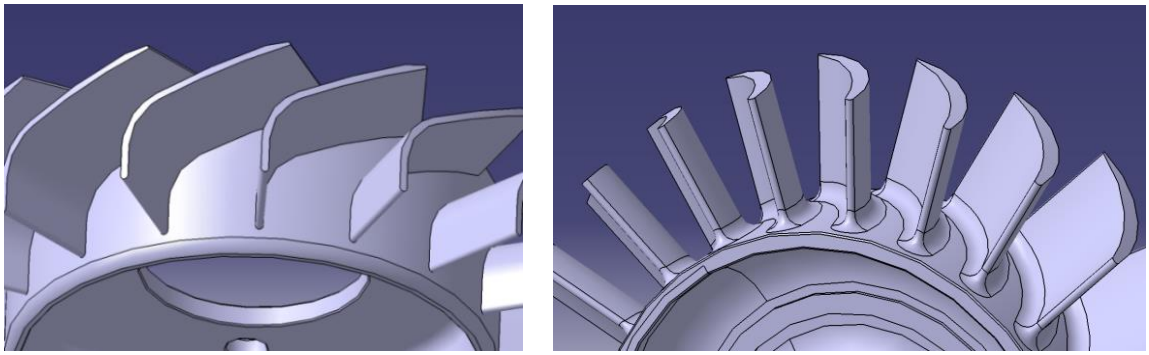

Fig. 2 Turbine baldes

In order to conduct numerical simulations, it was built in a CAD environment the complete working channel of the stage which represents the fluid domain, shown in Figure 3.

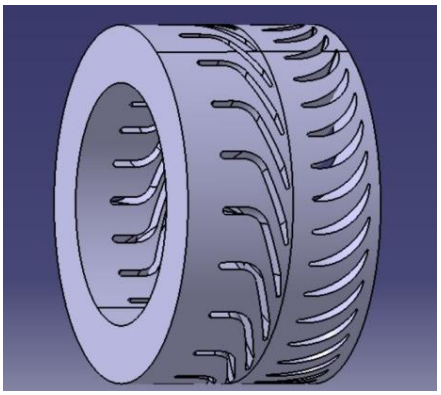

Fig. 3 Turbine fluid domain

3. NUMERICAL CALCULATION

The turbine studied in this paper consists of a single axial stage, its dimensions being reduced due to low mass flow, the nominal mass flow is approximative 0.685 kg/s, and high rotational speed, 80000 rpm nominal speed. The stator consists of 16 blades while the rotor has 23 blades, both of which consisting in cylindrical blades (the same profile over the entire height). To reduce the computation time and resources needed, the model was reduced to the flow channel formed by a stator blade and a rotor blade using the periodicity conditions available in the Ansys Workbench environment, Figure 4. The numerical grid used is unstructured, made of tetrahedra, with higher density of cells near the surfaces, having a number of 162548 elements, Figure 5.

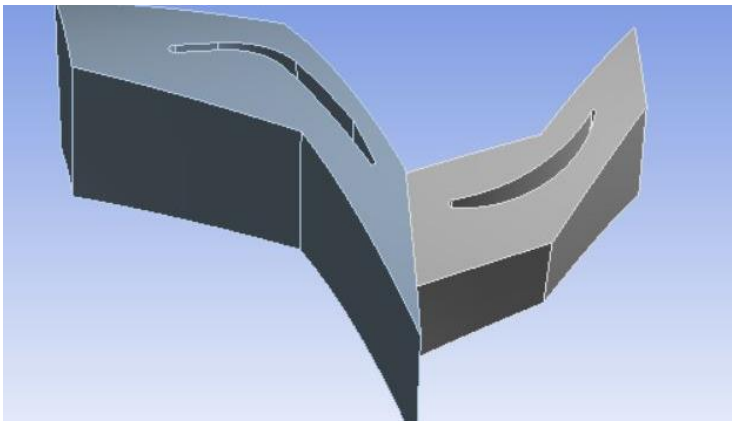

Fig. 4 Flow domain

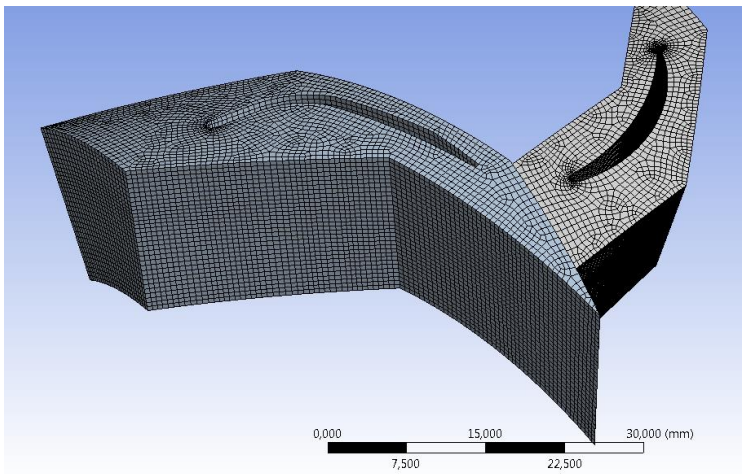

Fig. 5 Numerical grid

The input data for numerical simulation are taken from the calculation of the turbine engine thermodynamic cycle, thus the turbine must generate a power equal to that of the compressor at a higher efficiency, the conditions at nominal input being:

- total pressure: 472600 [Pa]
- total temperature: 1173 [K]
- mass flow: 0.685 [kg/s]

A large number of numerical cases have been solved, at rotational speeds ranging from 5000 to 100000 rpm, with a step of 5000 rpm. The working fluid was considered to be air as an ideal gas (the use of air as a working fluid instead of combustion gases does not introduce large errors due to the fact that the two specific gas constants are approximately equal). The mass flow was also varied with 10% from the nominal mass flow resulting in over 100 numerical cases. Two examples of the results obtained in Ansys CFX are shown in Figures 6 and 7.

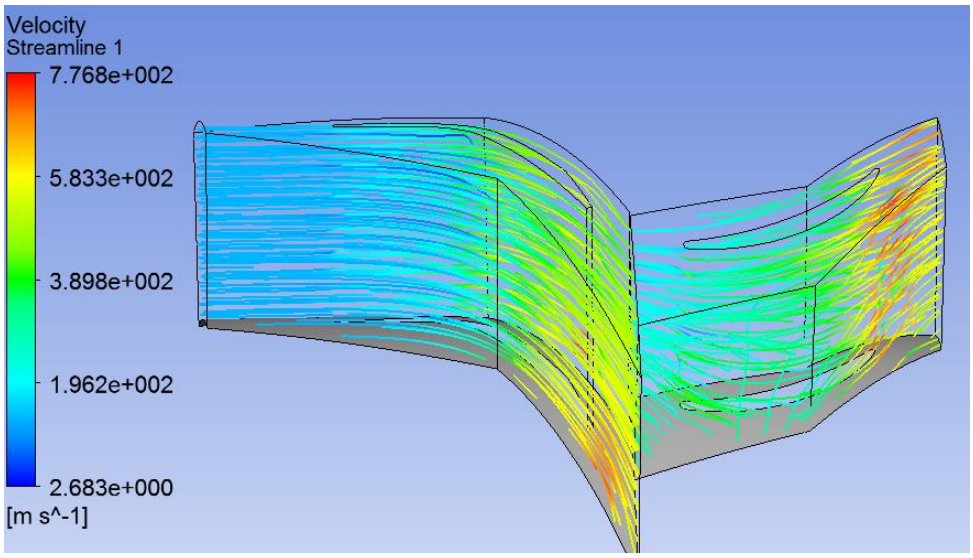

Fig. 6 Streamlines

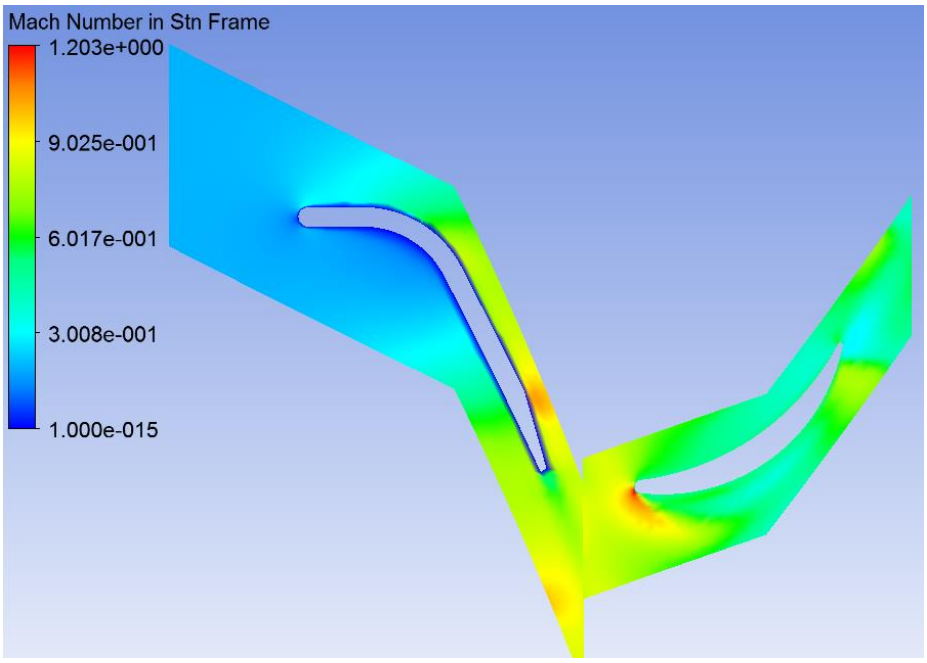

Fig. 7 Mach number distribution across the stage

The distribution of streamlines around the blades describes the flow in the working channel. A smooth flow without vortices results in a high turbine efficiency. Also, the distribution of streamlines and Mach number provides good indication of blade profile positioning.

4. TURBINE PERFORMANCE MAP

By definition, turbine performance map is the set of curves which comprise the variations in the expansion degree of the working fluid, represented by the variation of the total enthalpy in the turbine, relative to the inlet temperature, Δh^*_{Tred} and the adiabatic efficiency of the turbine, η^*_T, defined in terms of similarity parameters of mass flow and rotational speed.

Analytically, the universal feature can be expressed by:

$$\begin{cases} \Delta h^*_{Tred} = f\left(\dot{M}_g \dfrac{\sqrt{T_1^*}}{P_1^*}, \dfrac{n}{\sqrt{T_1^*}}\right) \\ \eta^*_T = f\left(\dot{M}_g \dfrac{\sqrt{T_1^*}}{P_1^*}, \dfrac{n}{\sqrt{T_1^*}}\right) \end{cases} \quad (1)$$

where the index "1" defines the turbine inlet section. [4]

The universality character is given by parameters of similarity, a single point on the characteristic representing a set of operating regimes. Similarity analysis has arisen in connection with the scientific activity of quantitative comparison of two or more different systems in which the same types of phenomena occur. Fluid mechanics has described four fundamental principles of similarity:

- Prandtl criterion, Pr = ct., generally characterizes non-adiabatic processes. As expansion is considered an adiabatic process, this criterion is inappropriate;
- Homocrony criterion, Ho, is characteristic of non-stationary processes, processes that are not described by this characteristic of the turbine, and therefore this criterion is also inapplicable;
- Reynolds criterion, Re = ct. In the case of real flow processes through turbomachinery, it has been found that the phenomenon is self-modeling in relation to the Reynolds number, therefore this criterion is not characteristic of flow through an axial gas turbine;
- Mach criterion, M = ct., is the only criterion of kinematic similarity that can be applied to flow processes through a gas turbine. For two values to be similar according to this criterion, the numbers must be invariants of similarity. To meet all the specifications of a kinematic similarity, it is necessary that all three Mach numbers, absolute, relative and transport speeds are constant. [5]

$$\begin{cases} M_u = ct. \\ M_w = ct. \\ M_c = ct. \end{cases} \quad (2)$$

With these invariants, the similarity parameters of speed and mass flow are obtained.

$$\frac{N}{\sqrt{T_1^*}} = ct. \quad (3)$$

$$\dot{M}_g \frac{\sqrt{T_1^*}}{P_1^*} = ct. \quad (4)$$

There are several possible types of approaches to construct the performance map of a turbine, each of them with advantages and disadvantages: theoretical, CFD and experimental. They can be used separately, but also together, in the desired combinations, for checking and validating the results.

Using the above-described grids, the k-e turbulence model and the frozen rotor simulation type, a multitude of results synthesized in Figure 8 was obtained.

The map was built by joining the points representing the numerical cases analysed. In order to determine a constant mass flow line, the following parameters were kept constant: mass flow, inlet temperature and pressure, and speed was varied ranging from maximum 100000 rpm (2919.78 rot/min/(K^1/2) in terms of reduced speed) by 5000 rpm. In order to determine the other constant mass flow lines, the mass flow was modified by 10% decrease. The minimum input mass flow for which the numerical calculations were performed is 50% of the nominal flow, a lower mass flow determines, as can be seen from Figure 9, a negative variation of the enthalpy on the turbine, which has no correspondent in reality.

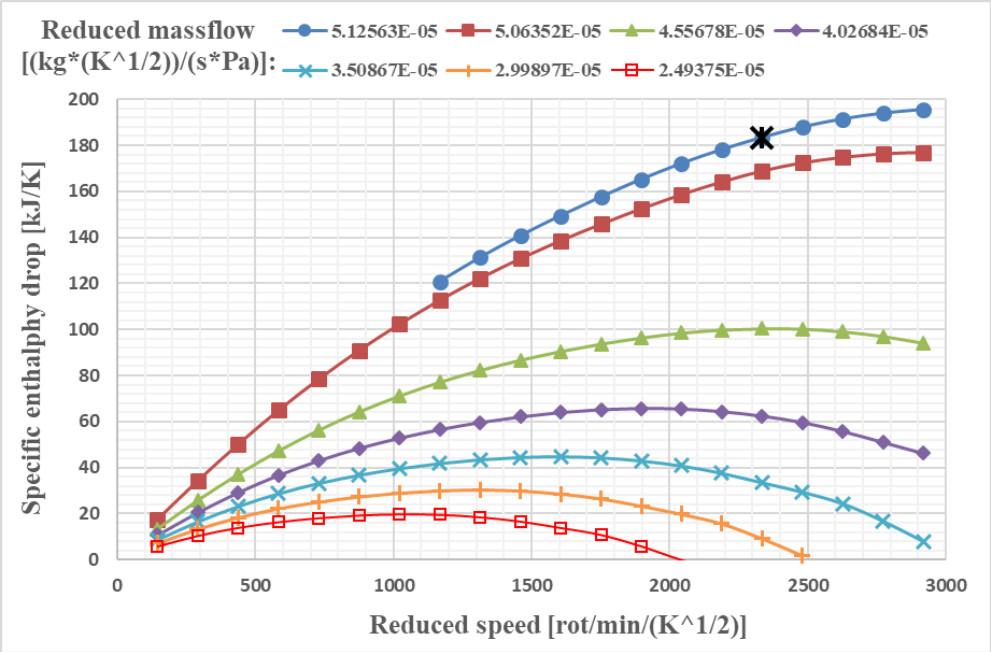

Fig. 8 The turbine performance map obtained by CFD calculations

Using the universal characteristic of the turbine, its performance can be determined at any operational parameters. It can be seen that an increase in speed causes an increase in the power produced by the turbine, expressed here by the specific enthalpy variation. But from a certain speed value, depending on the reduced mass flow, the increase in speed produces a decrease in turbine power.

The nominal engine regime is chosen so that the power developed by the turbine is equal to that required for the compressor. However, other factors such as: engine performance, compressor performance, turbine efficiency, mechanical loads and bearings have been taken into account in the choice of the nominal point. Thus, the speed of 80000 rpm (2335.8 rot/min/(K^1/2) in terms of reduced speed) was chosen as nominal speed.

Figure 10 shows the turbine efficiency characteristic, from which it can be seen that the efficiency varies in the same way with the speed. High efficiency is obtained at higher speed, but increasing speed past a certain amount will determine a decrease in turbine efficiency. It is recommended that the operation of the turbine follow points with the highest efficiency, but this depends on the performance of the compressor, the combustion chamber and the desired regimes.

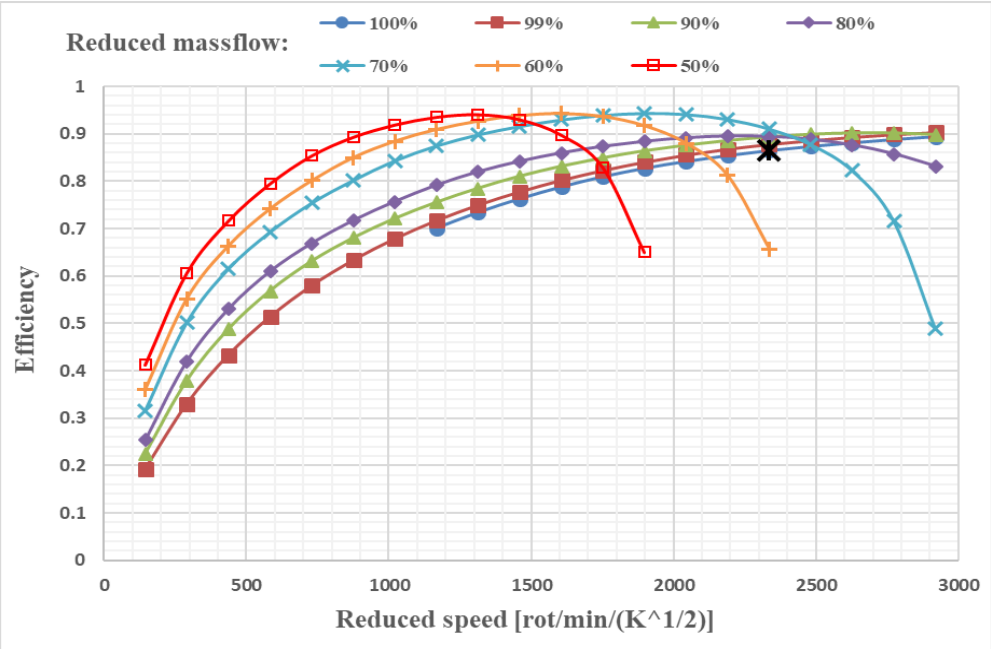

Fig 10. Turbine efficiency map

5. CONCLUSIONS

In this paper was presented a method for determining the theoretical performance map of an axial turbine using the numerical calculation of CFD type. The map was obtained using similarity parameters calculated using the results of multiple numerical cases. By modifying two parameters in the input conditions of the numerical simulation, the complete characteristic of the axial turbine was achieved. The obtained characteristics follow the form of the theoretical and experimental characteristics existing in the literature.

For future studies on theoretical characteristics determined by numerical computation, it is recommended to use a smaller number of numerical cases in order to reduce the workload and the time to neede to achieve the maps. It is possible to determine the theoretical map with satisfactory accuracy using about 5 cases for a constant reduced mass flow, instead of 20 cases used in this paper.

REFERENCES

[1] D. Olaru, V. Vilag, C. Cuciumita, J. Popescu, R. Mihalache, „Axial Turbine Gasodynamic Study", INAS Conference Sinaia, High Performance Computer Engineering Solutions, 19 – 21 May 2011 ISBN 978-973-0-11025-8

[2] Ainley, D. G. & Mathieson, G. C. R., "A Method of Performance Estimation for Axial-Flow Turbines", Aero Res Council Reports and Memoranda No. 2974, 1951

[3] Silivestru V., Ciolpan S., Tarbu D., Pirvulescu C & Dicu M., "Calculul caracteristicii turbinei generatorului de gaze - Motor Tp1", Documentatie Tehnica Increst, Dt100/90

[4] Virgil Stanciu, Carmen Mohnoghitei & Evelina Rotare, „ Carcteristicile turbomotoarelor", Editura BREN, Bucureşti, 2004, ISBN: 973-648-230-8

[5] Dunham, J. & Came, P. M., "Improvements to the Ainley-Mathieson Method of Turbine Performance Prediction", Trans. ASME Journal Eng. For Power, Vol. 92, 1970, Pp. 252-256

AERODYNAMIC AND AEROACOUSTIC IMPROVEMENTS OF VERTICAL AXIS WIND TURBINES USING SUPERCIRCULATION FLOW CONTROL

Dan Paul RADULESCU[1], Marius DEACONU[1]

ABSTRACT: Coflow-Jet (CFJ) represents a new supercirculation flow control method able to improve the aerodynamic performance of the airfoils due to increased circulation on the suction side. Operating wind turbines generate tonal and broadband noises affecting the living environment adversely; especially small wind turbines located in the vicinity of human living places. The current study carries out numerical prediction for aerodynamic performance and noise radiated from an H-Darrieus Vertical Axis Wind Turbine which uses CFJ. Incompressible transient simulation is conducted to obtain the instantaneous turbulent flow field. Noise prediction was performed by the Ffowcs Williams and Hawkings (FW–H) acoustic analogy formulation. Simulations were performed for three different tip-speed ratios (TSR). First, the mean torque coefficient is compared with the basic VAWT which does not use CFJ. Then, the study focuses on the broadband noises of the turbulent boundary layers and the tonal noises due to blade passing frequency.

KEYWORDS: aeroacoustic, CFJ, supercirculation, momentum, URANS

NOMENCLATURE

AoA	-	angle of attack
CFJ	-	coflow-jet
CL,Cd,CM	-	Lift,Drag,Momentum coeficients
HAWT	-	horizontal axis wind turbine
LE	-	leading edge
TE	-	trailing edge
TSR	-	tip speed ratio
VAWT	-	vertical axis wind turbine

1. INTRODUCTION

There are two main types of VAWT depending of the force type generated by the blades: Lift type and Drag type. Lift type are generally considered more efficient and closer to the efficiency of HAWT [1]. The blade section of VAWT, unlike HAWT, is subjected to unsteady variation of angle of attack. This variation is a function of tip speed ratio (TSR) and is higher when TSR is lower. A dynamic stall phenomenon appears when angle of attack exceeds the static stall angle. This decreases the aerodynamic performance and represents an important aerodynamic noise source [1,2,3,4]. Another specific feature of VAWT is the interaction between the blades with the wake produced by the other blades which is convected through the rotor. This interaction produces fluctuating lift and represents an important aeroacoustic noise source both tonal and broadband [5,6]. In order to reduce these negative features, there is a strong demand to develop flow control methods which can reduce both dynamic stall and the wake. Several flow control methods have been investigated for wind turbines like trailing edge flaps (Lee et al.,2013), blowing jets (Wang et al.,2013), Gurney flaps (Tongchitpakdee et al.,2006), plasma actuators (Greenblatt,2014) aso. Results showed some improvements of aerodynamic performance but at a cost of technological complexity. An interesting airfoil flow control concept was developed by Zha et al. (2004). This paper numerically evaluates the aerodynamic and aero-acoustic performance when this concept is applied to a lift type VAWT.

[1] Romanian Research and Development Institute for Gas Turbines COMOTI, Department of Acoustics and Vibration

2. DYNAMICS OF VAWT

The aerodynamics of a lift-type VAWT are fundamentally unsteady. As the blade rotates around the hub the angle between the blade velocity and the wind velocity varies significantly. This creates a variation in angle of attack and hence a variation in the aerodynamic forces exerted on the blades. The magnitude of this variation is governed by the tip speed ratio (TSR) which is defined as the ratio of the blade speed to the wind speed. An approximation of the variation in blade angle of attack can be calculated using simple geometry by assuming that the free stream flow is uniform in both magnitude and direction over the whole rotor. This 'geometric' variation in angle of attack is shown in Fig. 1 for a range of TSR [7]. It is important to note that the geometric angle of attack varies from the true angle of attack due to the deflection of the incoming flow by the rotor.

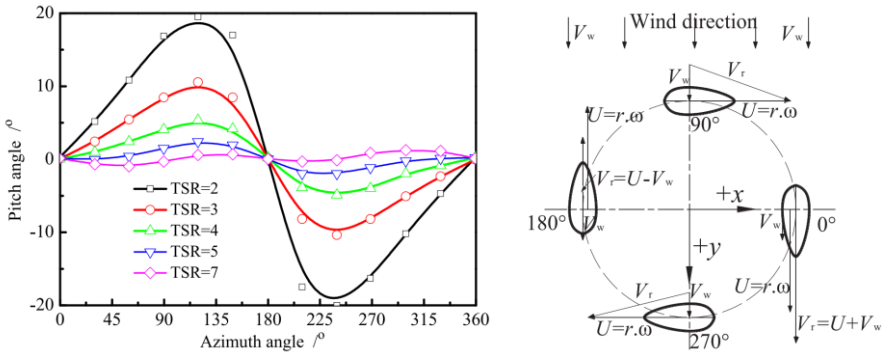

Fig. 1 Blade angle of attack variation [7]

The second key feature of VAWT operation is the fact that the blades in the upstream half of the rotation shed a wake that passes through the rotor and interacts with the blades in the downstream half of the rotation. This potentially introduces further unsteady blade loading that could affect the noise radiated by VAWT rotor.

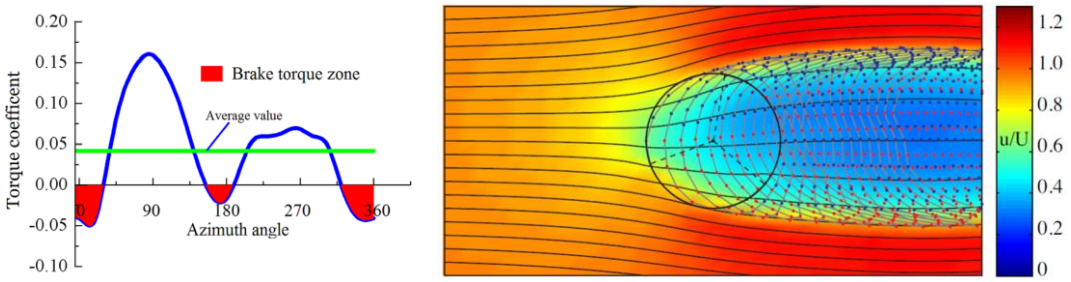

Fig. 2 a) One blade momentum during 1 cycle [7], b) Velocity field around VAWT (McIntosh,2013)

A typical torque graph produced by one blade during a full 360 ^{0} cycle is presented in Fig. 2 a). It can be seen that most of the power is produced within from half cycle where the kinetic energy extraction is maximum. The remaining flow has a smaller average velocity due to this blockage effect as can be seen in Fig. 2 b).

2.1. Aeroacoustic noise sources

Aeroacoustic noise sources of a VAWT include several categories which produce both tonal and broadband noise. The most important are considered: dynamic stall, blade- wake interaction and incoming turbulence –blade interaction. The use of supercirculation as CFJ should reduce at least two important noise sources: dynamic stall and blade-wake interaction.

2.2. Coflow-Jet supercirculation principle

CFJ method [8] consists in adding injection slots near the leading edge and suction slots near the trailing edge of a basic airfoil, as in Fig. 3. Air is injected near the LE and extracted near the TE using a recirculation pump, so we have the case of zero net mass flux since the mass of injected air is equal with the extracted mass.

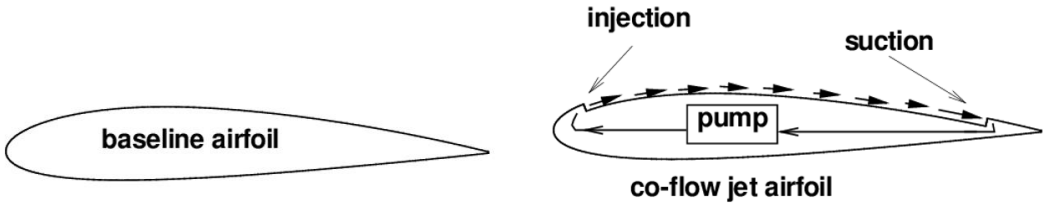

Fig. 3 CFJ principle [8]

The aerodynamic results of such circulation are: increased boundary limit momentum, much higher stall AoA, decreased wake, much higher lift and a reduced induced drag. It must be mentioned that for some configurations it is possible to achieve even a negative induced drag which makes the solution highly attractive for new airplanes design. A typical performance graph showing Lift and Drag coefficients of CJF and baseline airfoils are presented in Fig. 4. From an aeroacoustic point of view, the delayed stall produces less wake behind the profiles so it was expected that in case of VAWT to find a decrease of the blade-wake interaction noise

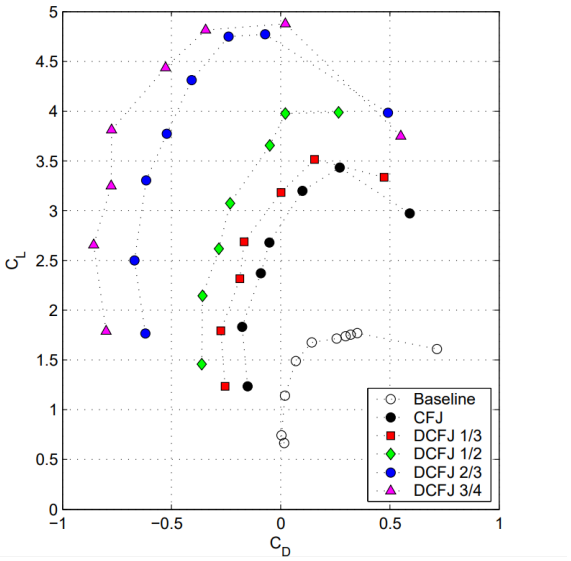

Fig 4 Performance curves for CFJ airfoils [9]

2.4 Numerical aerodynamic and aeroacoustic simulation

2.4.1 Geometry and mesh

Numerical 2 D study was conducted on 3 blades, H-type VAWT with the following characteristics: R= 1.2 m; Basic blade profile NACA0021 with C=0.3 m. For CJF modified profile we used: hinjection slot = 0.002 m; hsuccion slot =0.004 m. Injection and suction slots are placed at 6% chord and 80% chord distance from the leading edge as can be seen in Fig. 5.

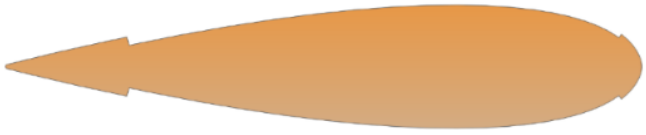

Fig. 5 Airfoil design with CFJ on both sides [10]

Injection and suction slots were used on both sides of the airfoils due to the fact that during a complete rotation the angle of attack oscillates between negative and positive values so the suction side becomes pressure side. It should be mentioned that it is possible to use active control of the jets in order to use them alternatively only for the suction side. The domain was divided in 3 circular parts, two static and one rotating containing the turbine blades (as seen in Fig. 6). Mesh was structured for the static domains and partially structured for the rotating domain. We used a number of 845000 cells and 853000 nodes. For the boundary layer we used an y+ = max. 2.2 which was calculated after the simulation. Total domain D1 diameter was 6 times the VAWT diameter in order to keep the acoustic sources information inside.

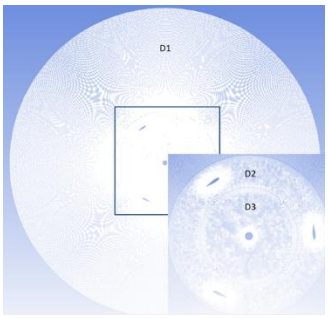

Fig. 6 Numerical mesh

2.4.2 Numerical algorithm

Numerical simulation for aerodynamic and acoustic field was conducted with Ansys Fluent software. For the aerodynamic analysis, we used URANS and SST turbulence model. Transitory analysis was made using an implicit scheme using a time step which correspond to 1 degree of rotation. Every time step was iterated by 20 times. In the current paper, the discretization algorithm was conducted by SIMPLE with second-order upwind scheme by under-relaxation factors for ensuring convergence of iterative computations. The transient formulation was performed by second order implicit. Simulations were performed for Basic and CFJ airfoils at TSR 1.5; 2; 2.5. Injection and suction mass flow were established for each TSR in order to have no stall at maximum angle of attack for that configuration. This resulted from separated steady flow RANS simulations using CFJ airfoils at different attack angles and flow speed. This resulted in the minimum injection mass flow which was later used as a boundary condition for the VAWT simulation.

2.4.3 Boundary conditions

Table 1. Boundary conditions

Parameter	Value
Incoming far field velocity	10 m/s
Turbulent intensity far-field	5%
Flow density	1.225 kg/m^3
Dynamic viscosity 1.789x10^{-5}	1.789 x 10^{-5} Ns/m^2
Turbulent intensity injection –suction slots	5%
Injection speed	90 m/s
Suction speed	45 m/s
Walls	Non-slip condition

2.5 Results

2.5.1 Aerodynamic performance

The use of CFJ for the VAWT increases the output power by reducing or completely eliminating the stall of the airfoils and due to the reactive force which appears due to the jets. However, this performance comes to a cost, which is the power consumption of the jets which must be evaluated and subtract it from the overall generated power by the VAWT. Since the study was dedicated to the acoustic field, this evaluation was not conducted here. Data and results regarding the Momentum coefficient (CM) and the comparison between Baseline (no jet) and CFJ solution for TSR 1.5; 2; 2.5 are presented below.

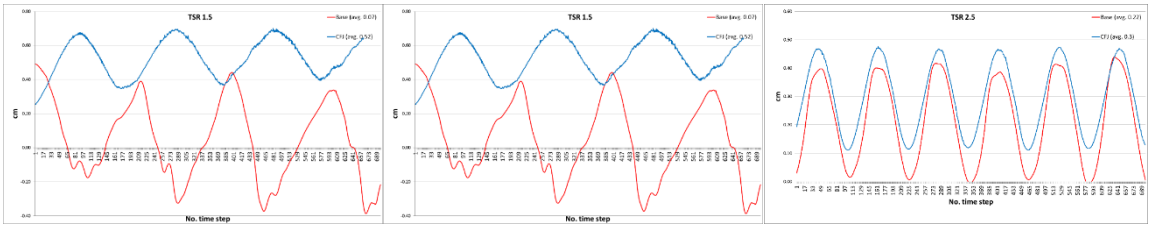

Fig. 7 Momentum coefficient for different TSR values

Aerodynamic performance is dramatically improved by CFJ solution especially for low TSR. It is worth to mention that this performance is achieved by using a supplementary power to inject the air.

However, it has been previously demonstrated that it is possible to achieve a net gain using the CFJ as a super circulation method.

2.5.2 Aeroacoustic performance

The acoustic field around the wind was calculated using the Ffowcs Williams-Hawkings analogy. We distributed 8 receivers around the turbine at 3 m distance from the rotating axis as can be seen from Fig. 11. OASPL values for each receiver were calculated for TSR 1.5 ;2; 2.5 and are presented within Table 2. The values were calculated for overall frequency domain (0-600 Hz), infrasound (0-20Hz) and sound (20- 600 Hz) comparing Base with CFJ solution.

Table 2. Average OASPL

Configuration	Sound pressure level [dB]	**Frequency domain**					
		0-600 Hz		0-20Hz		20-600 Hz	
		Base	CFJ	Base	CFJ	Base	CFJ
TSR 1.5	Lp avg	104.5	102.7	104.3	102.6	88.6	86.3
	Diff		1.8		1.8		2.3
TSR 2	Lp avg	104.7	103.4	104.6	103.4	88.3	84.6
	Diff		1.3		1.3		3.7
TSR 2.5	Lp avg	104.8	99.2	104.7	99.1	90.1	81.2
	Diff		5.6		5.5		8.9

It can be seen that it is possible to achieve an important noise reduction on all frequencies and even more on audible domain. The max average reduction of 8.9 dB was obtained for TSR 2.5 case. The explanation might be that for this TSR the jets speed was optimised in order to be the minimum speed at which stall is not present.

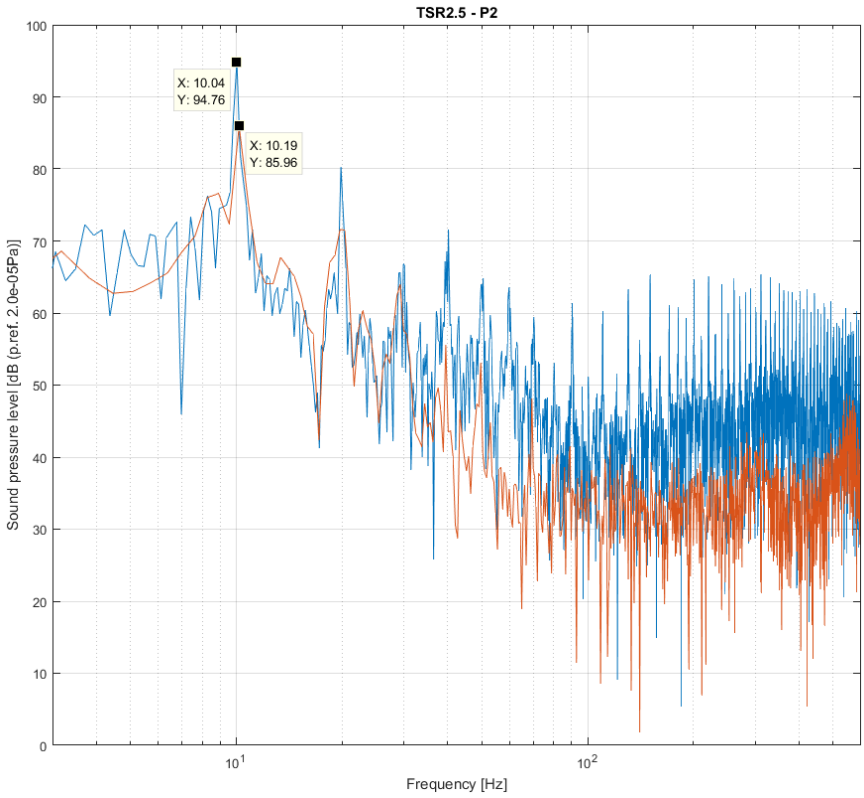

Fig. 8 Frequency domain for base and CFJ solutions at TSR 2.5

For smaller TSR it is possible that the jets were to strong and can add some broadband jet noise. An interesting finding is that CFJ is capable to strongly reduce the tonal noise as can be seen from the FFT analysis at receiver P2 and presented in Fig. 8. This was an expected result since the wake reduction due to CFJ reduces also the blade-wake interaction which is the main tonal noise source.

3. CONCLUSIONS

CFJ VAWT represents an interesting option for wind energy harvesting since it is efficient and quieter. Efficiency is much higher than the base but requires additional input power to recirculate the jet. However, it has been demonstrated by other authors that it is possible to achieve an important net gain in power output. Several interesting findings about noise field have been revealed by this study. The most important is that it is possible to get a strong OASPL reduction both broadband and tonal. This is the effect of wake reduction and thus the blade-noise interaction using CFJ supercirculation method. These findings require a future investigation for the possibility of optimization the CFJ VAWT in terms of aerodynamic efficiency and noise production.

ACKNOWLEDGEMENT

We would like to thank INCDT COMOTI for the resources provided, PhD eng. Romulus Petcu for advice and for acquiring the devices within "Nucleu" Program TURBOPROP, project number PN19.05.02.03.

REFERENCES

[1].Paraschivoiu I.,Saeed F., Desobry V.; 2002; Prediction capabilities in vertical axis wind turbine aerodynamics; The World Wind Energy Conference and Exhibition; Berlin, Germany;

[2].Castelli M.R.; 2012; Effect of blade number on a straight – bladed vertical axis Darrieus wind turbine; World Academy of Science, Engineering and Technology International Journal of Aerospace and Mechanical Engineering, vol.6; No.1 ; pg. 68 – 74;

[3].Ferreira S., Bijl H., G. Van Bussel,G van Kuik; 2007; Simulating dynamic stall in a 2D VAWT; Journal of Physics, Conference Series; vol. 75;

[4].RK Amiet; 1976; Noise due to turbulent flow past a trailing edge; Journal of Sound and Vibration; vol. 47; pg. 387-393;

[5].T Brooks; 1993; Studies of blade-vortex interaction noise reduction by rotor blade modification; NASA STI/Recon Technical Report A, 959:90093. ix, 29;

[6].M Castelli, A Villa, and E Bernini; 2011; CFD Analysis of the Influence of Central Shaft on Vertical Axis Wind Turbine Noise Emission; In International Wind Turbine Noise Conference, Rome, 52, 56;

[7] Z. Zhao, S. Qian, T. Wang ; 2017; Study on variable pitch strategy in H-type wind turbineconsidering effect of small angle of attack; Journal of renewable and sustainable energy; vol. 9;

[8].Zha, G.C. and Paxton C. ; 2004; A Novel Airfoil Circulation Augment Flow Control Method Using Co-Flow Jet; AIAA Paper 2004-2208, 2nd AIAA Flow Control Conference, Portland, Oregon.

[9] Zha G.; 2015; Ultra-High Efficiency Co-Flow Jet Airfoil and the Transformative Aircraft; AIAA Paper 2016-3207; 12 th AIAA Flow Control Conference; Austin,Texas.

[10] Radulescu et al.;2019; Numerical study of aerodynamic radiated noise of a Coflow-Jet Vertical Axis Wind Turbine; 8th International Wind turbine noise Conference, Lisbon, Portugal

8th European Aeronautics Days

27 - 30 May, 2019

Bucharest, Romania - Palace of the Parliament

Europe's Technological Achievements for a Sustainable Future of Aviation

AERODAYS - the leading European event in aviation research and innovation, a solid platform to share and review that latest developments in aeronautics and air transport across the European Union.

Launched in 1991, Aerodays celebrates its 8th edition with an innovative concept, TandemAERODays19.20, based on two integrated events organized in Romania, in 2019, and Germany, in 2020, while Bucharest is the first Aerodays host in Central and Eastern Europe.

STRATEGIC OBJECTIVES FOR BUCHAREST

Bucharest AERODays 2019 promotes regional policies for research and education in aeronautics.

It aims was to facilitate and encourage the participation of Eastern European countries to a high-level event to share their expertise in specific areas of industrial competitiveness.

It offers a platform for the dissemination and implementation of world-leading EU projects and technical programs based on the Horizon 2020 framework.

Provides communication links between European companies, from small and medium-sized enterprises to multinational companies, and nurtures a fruitful exchange of ideas with the research community.

COMOTI

The only specialized company that integrates such activities as

scientific research,
design,
manufacturing,
testing,
experimental activities,
technologic transfer and innovation

in the field of aircraft and industrial gas turbines and high speed bladed machinery.

220D Iuliu Maniu Ave., 061206 Bucharest, ROMANIA,
P.O. 76, P.O.B. 174
Phone: (+4)021/434.01.98, (+4)021/434.02.31, (+4)021/434.02.40
Fax: (+4)021/434.02.41, e-mail: contact@comoti.ro

www.comoti.ro